Bioluminescence in a complex coastal environment: 1. Temporal dynamics of nighttime water-leaving radiance

Mark A. Moline
Biological Sciences Department, California Polytechnic State University,
San Luis Obispo, California, USA

Matthew J. Oliver
Coastal Ocean Observation Laboratory, Institute of Marine and Coastal Sciences, Rutgers University,
New Brunswick, New Jersey, USA

Curtis D. Mobley and Lydia Sundman
Sequoia Scientific Inc.,
Bellevue, Washington, USA

Thomas Bensky
Biological Sciences Department, California Polytechnic State University,
San Luis Obispo, California, USA

Trisha Bergmann
Coastal Ocean Observation Laboratory, Institute of Marine and Coastal Sciences, Rutgers University,
New Brunswick, New Jersey, USA

W. Paul Bissett
Florida Environmental Research Institute,
Tampa, Florida, USA

James Case
Marine Science Institute, University of California,
Santa Barbara, California, USA

Erika H. Raymond
Ocean Research & Conservation Association,
Fort Pierce, Florida, USA

Oscar M. E. Schofield
Coastal Ocean Observation Laboratory, Institute of Marine and Coastal Sciences, Rutgers University,
New Brunswick, New Jersey, USA

Abstract

Nighttime water-leaving radiance is a function of the depth-dependent distribution of both the in situ bioluminescence emissions and the absorption and scattering properties of the water. The vertical distributions of these parameters were used as inputs for a modified one-dimensional radiative transfer model to solve for spectral bioluminescence water-leaving radiance from prescribed depths of the water column. Variation in the water-leaving radiance was consistent with local episodic physical forcing events, with tidal forcing, terrestrial runoff, particulate accumulation, and biological responses influencing the shorter timescale dynamics. There was a >90 nm shift in the peak water-leaving radiance from blue (~474 nm) to green as light propagated to the surface. In addition to clues in ecosystem responses to physical forcing, the temporal dynamics in intensity and spectral quality of water-leaving radiance provide suitable ranges for assessing detection. This may provide the information needed to estimate the depth of internal light sources in the ocean, which is discussed in part 2 of this paper.

Keywords: bioluminescence, water-leaving radiance, optics.

Introduction

Bioluminescence in the ocean is the result of biologically generated photons from a chemiluminescent reaction. It is produced by over 700 genera representing 16 phyla, spanning the range of small single cell bacteria to large vertebrates [Herring, 1987]. The reasons for these luminous displays appear to be as varied as the organisms themselves, but may be divided into basic categories of predator avoidance, prey attraction, and intraspecies communication [Burkenroad, 1943; Abrahams and Townsend, 1993; Morin, 1983; Morin and Cohen, 1991]. A ubiquitous feature of most of these organisms is that mechanical stimulation will cause these organisms to generate light, which often leads to brilliant displays in the wakes of ships, in breaking waves, or even around the bodies of rapidly moving dolphins [Rohr et al., 1998]. Emission characteristics vary according to organism, most (i.e., bacteria, dinoflagellates, copepods) with peak emission between 440 nm and 500 nm [Hastings and Nealson, 1977; Miller et al., 2005], and depend on the luciferin structure and reaction substrates [Hastings, 1983]. Bioluminescent displays generate wonder and curiosity, and early research on this phenomenon was driven primarily by the desire to understand the physiological mechanisms of bioluminescence, as well as the ecological advantage that bioluminescent abilities provides to these luminous organisms [Alberte, 1993].

Aside from the basic desire to understand the organism-specific bioluminescence potential and ecological advantage, the fact that these organisms produce light upon mechanical stimulation is of military interest. Light production as a function of mechanical stimulation provides a direct visual method of identifying surface and subsurface vessels and swimmer tracks. The development of a passive method (as opposed to active methods such as RADAR or LIDAR) of identifying hostile ships, submarines, and swimmers, as well as the development of strategies to reduce the risk of detection are relevant [Lynch, 1981; Lapota, 2003, 2005]. Support for marine bioluminescence research in the last 40 years reflects this relative importance [Nealson, 1993].

Over the years, a qualitative understanding of the distribution and intensity of Mechanically stimulated Bioluminescence Potential (MBP) has been acquired. MBP generally refers to the flash potential from a single stimulus event measured in a chambered pump-through bathy-photometer (BP) [Seliger et al., 1969]. In general, bioluminescence potential in the epipelagic zone is directly related (with a large variance) to total biological biomass loads and/or eutrophication of the water column [Lapota, 1998]. The organisms responsible for the majority of the MBP appear to be either mixotrophic or heterotrophic and include dinoflagellates, copepods, ostracods, euphausiids, larvaeceans, and gelatinous zooplankton [Herring, 1987]. The dominance of MBP by a set of organisms might lead one to suspect an ecological mechanism might be highly correlated with MBP. Such a correlation would yield a quantitative relationship that could be used to predict MBP and provide a valuable tool.

The Biowatt and Marine Light-Mixed Layer (MLML) programs were the first large-scale attempts to relate physical oceanography to the optical and bioluminescence variability of the water column [Marra and Hartwig, 1984]. Results from these and subsequent programs illustrate that a predictive relationship is difficult to develop [Marra et al., 1995], as the MBP is rarely dominated by a single group of organisms and is regulated by the dynamics of growth, grazing, behavior, senescence, and differences in flash intensities [Lapota and Losee, 1984; Lapota et al., 1988, 1989, 1992; Batchelder et al., 1990, 1992; Swift et al., 1995]. Additional complications for simplistic relationships arise from the dynamics of physical forcing. In particular, bioluminescent organisms are frequently found at convergence zones between water mass boundaries, including both horizontal (e.g., fronts [Moline et al., 2001; Cussatlegras et al., 2001]), and vertical boundaries (e.g., thin-layers [Widder et al., 1999]). They may also accumulate in coastal environments as a result of the interaction between vertical migration and convergent physics

[Franks, 1992a, 1992b, 1995; Franks and Chen, 1996]. These ecological and physical complications, as well as differences in measurement techniques [Case et al., 1993], have made the derivation of robust direct relationships of MBP to environmental conditions very difficult to achieve.

Biowatt and MLML were also some of the first programs to recognize the importance of an accurate description of the optical properties of the water column in both of the propagation of light in the water column and the ecological structure of the water column [Smith et al., 1989; Dickey et al., 1993; Carder et al., 1995; Ondercin et al., 1995; Stramska et al., 1995]. As stated, the accumulations of bioluminescent organisms are an ecological response to the physical, chemical, and biological forcing of the marine system, which includes the feedback of the time dependent change in the Inherent Optical Properties (IOPs). The applied risks and opportunities from bioluminescence radiance are also directly a function of the IOPs, as the propagation of bioluminescence radiance through the air-sea surface is dependent on the attenuation and spread of the signal as it moves through the water column [Gordon, 1987]. Knowledge of the MBP alone may be less than useful if the probability of the bioluminescent photons escaping the water and being detected is unknown. In addition, the pioneering work of Biowatt and MLML helped focus the oceanographic community on the importance of spectral determination of the optical properties and its concomitant impact on spectral light transmission, rather than broadband light attenuation measurement, i.e., photosynthetically active radiation (PAR). These broadband measures were frequently much different than those at the specific wavelengths, and result in different estimations of water-leaving radiance from solar radiation and/or a bioluminescence event.

Here we present two time series data sets of the combined measures of MBP and IOPs for the estimation of bioluminescence water-leaving radiance (BL_w). The temporal dynamics of MBP and IOPs will be discussed in the context of local physical forcing and biological response. With these data, the integrated BL_w, generated by a modified radiative transfer equation (RTE) model, is solved simultaneously from all depths. BL_w will illustrate the contributions of the input variables to the variability in the overall signal and allow discussion of the commonalities between the two data sets collected in different years. This quantitative approach also takes into account the variability in the spectral light field, which provides additional information about the BL_w and the depth of a particular light source. Important to this discussion will be the recognition that the applied interest in BL_w is driven primarily by the opportunities and hazards that result from bioluminescent events, and a path toward sensing and prediction of these events in the ocean, the topic of part 2 of this paper [Oliver et al., 2007].

Methods

---INSERT FIGURE 1---

Two data sets were collected in 2000 and 2001 for this study as part of a larger Hyperspectral Coupled Ocean Dynamics Experiments (HyCODE) program, designed to utilize hyperspectral imagery to improve understanding of the diverse processes controlling IOPs and the influence of changing IOPs in the coastal ocean. Both data sets were collected using robotic vertical profilers. The profilers were deployed 10 km offshore of the New Jersey coastline in 14 m of water at 39°27.41 N, 74°14.75 W (Figure 1). The profiler frames were anchored to the seafloor with instrument packages attached to a floating drogue which was depth controlled by an attached winch (Figure 1). One vertical profiler, known as the Long-term Ecosystem Observatory or LEO-15, provided temperature and salinity using a Seabird 911 CTD as well as power and data transfer capabilities to the second profiler and to shore via an electro

fiber-optic cable. Relevant to this study, the second profiler instrument package consisted of a Wetlabs ac-9 absorption and attenuation meter at nine wavelengths (412, 440, 488, 510, 532, 555, 650, 676 and 715 nm), a HOBI Labs HydroScat-2 backscatter/fluorometer at two wavelengths (470 nm and 676 nm), and a bioluminescence BP [Herren et al., 2005; Moline et al., 2005]. A centrifugal-type impeller pump drives the water into an enclosed 500 ml chamber in the BP section, where a light-baffled Hamatsu H5783 photomultiplier tube measures stimulated bioluminescence between 300 and 650 nm. The inside of the chamber is coated with a 0.075 mm flat white coating to maximize the amount of stimulated light measured by the PMT. The effective detection limit due to gain settings and the A/D conversion was 1×10^6 photons L^{-1} s^{-1}. As the water passes into the detection chamber, the impeller pump creates turbulent flow, which mechanically stimulates bioluminescence. The flow rate through the chamber is dependent upon the rotation rate of the impeller rotor. This rate is adjusted to achieve residence times of 1.2 s–1.4 s, or flow rates of approximately 400 ml s^{-1}. A flowmeter monitors pumping rates using a magnet and a Hall Effect sensor to generate a period signal, which is converted to an analog signal of flow rate. The flow rates are measured as the water passes from the detection chamber to exhaust outlet. The BP was calibrated before and after each deployment with a known LED light source entering the PMT chamber. There were no significant differences in the measured light before and after each experiment for either year. The ac-9 and HydroScat-2 were factory calibrated and the ac-9 was clean water calibrated prior to the profiler deployment each year. While IOP data were collected continually during the experiments, bioluminescence data were only collected during nighttime profiles (2100-0500) local time. In 2000, the profiler was deployed for ~15 days logging 339 nighttime profiles while in 2001, it was deployed for ~8 days logging 132 nighttime profiles. Ten meter elevation wind velocities from the Rutgers University Marine Field Station were also measured over the study for estimation of sea surface roughness for the RTE model input.

Data Treatment

Data from the field instruments were quality controlled and formatted for the RTE model. Absorption data were integrated with concurrently collected temperature data and were temperature [Pegau et al., 1997] and scattering corrected [Zaneveld and Kitchen, 1994]. Because of the abundance of gelatinous zooplankton in the water column, ac-9 data were filtered using a moving mean of five data points to remove spurious spikes in the data. This removal of data from this filtering approach was rare and represented less than 2% of the total data set. Absorption, attenuation, backscatter, and volume scattering data were then depth merged into 0.25 m bins.

Radiative Transfer Model

To quantify the impact of IOPs and bioluminescence on spectral BL_w (380–700 nm), a new bioluminescence module was integrated into the HydroLight v. 4.2 RTE model [Mobley and Sundman, 2001a, 2001b] (http://www.hydrolight.info). The model settings used 0.25 m binned absorption, attenuation, backscatter, as well as measured wind speeds to estimate sea surface roughness. Model runs used pure water absorption values by Pope and Fry [1997]. The volume scattering function was estimate from the measured bb/b according to Petzold [1972]. The HydroLight model computed a new spectral scattering phase function when the backscatter to total scatter ratio (bb/b) changed by more than 0.005. Default atmospheric parameters (except wind speed) were used for all runs, with the user defined irradiance field input set to zero to simulate nighttime conditions. The bottom depth was set at 14 m and was assumed to be opaque. The inputs for this application were measured IOPs, thus we avoided using concentrations of seawater components such as chlorophyll and colored dissolved material (CDOM) in bio-optical IOP models. HydroLight has a user option to include bioluminescence as an internal light source in the model run. For this study, however, a new module was written to allow bioluminescence data to be a user input parameter, as are the IOP inputs, and to distribute these photons for propagation in the water column. The model was layered into 1 m sections to simulate stimulation of the bioluminescent organisms on a realistic scale in an applied sense. These specific locations in the water column (1 m thick

in this case) were sequentially "stimulated" in each model run, rather than the entire water column at once. This layering approach decomposed each bioluminescence profile into thirteen 1 m sections and allowed for the calculation of surface BL_w of the entire water column if only discrete portions of the water column were emitting bioluminescent light. An example of this data processing is as follows.

--- INSERT FIGURE 2 ---

--- INSERT FIGURE 3 ---

As bioluminescence spectra are known to vary with organism [Latz et al., 1987, 1988], profiles of bioluminescence were spectrally reconstructed for each measurement using known spectra from a range of dinoflagellate and copepod bioluminescence emission spectra (Figure 2). For this study the spectral shape of the bioluminescence emission spectrum consisted of 37 wavelengths from 380 nm to 680 nm. The model read each bioluminescence value at the depth of measurement and converted the photon counts into spectrally dependent energy ($W\ m^{-3}\ sr^{-1}\ nm^{-1}$). This energy appears as a source term in the RTE as solved by HydroLight [Mobley, 1994, equation [5.107]]. For each meter of every profile, the bioluminescence was then propagated upward through the surface waters for the 37 wavelengths using concurrently measured values of spectral absorption, attenuation, scattering, backscattering and sea state conditions as inputs into HydroLight. IOPs from the from the shallowest depth bin were propagated to the surface. An example from one model simulation is shown in Figure 3, with the "stimulation" of bioluminescence occurring between 6 m and 7 m depth. As the BL_w was calculated for each meter, requiring a different set of input files, a separate HydroLight run was needed for each condition. For this study, 7490 HydroLight runs were conducted to estimate the spectral BL_w for the 2000 and 2001 experiments.

Results

Temporal Dynamics in Environmental Variables

--- INSERT FIGURE 4 ---

Vertical distributions of density from 2000 showed a range of conditions, from strongly stratified layers to homogeneous distributions (Figure 4a). These conditions changed on timescales of days to weeks, representative of the local atmospheric forcing and the cycle of upwelling and downwelling that characterizes the region along the New Jersey coast [Glenn et al., 2004]. Upwelling conditions are generated by southwest winds that move the warm surface waters offshore and entrain colder high salinity waters from deeper waters of the shelf. During a downwelling condition, this warm surface layer is pushed toward the coast, effectively removing stratification in the water column [Moline et al., 2004]. Over the 2000 deployment there were two periods of downwelling and two upwelling (Figure 4a). Initial downwelling was followed within a day by an intense upwelling period peaking on 22 July 2000. A change in the water mass was evident during the second downwelling condition on 27 July 2000, characteristic of influence of the Hudson River plume which periodically extends south along the New Jersey coast [Oliver et al., 2004]. The final days of the deployment were characterized by upwelling conditions, which established a stratified water column. The optical variability followed the physical dynamics, with low attenuation associated with the entrained upwelled water (Figure 4b). Beam attenuation at 488 nm (c488), near the peak bioluminescence emission wavelength (Figure 2), in the warm surface layer increased toward the end of the deployment to over 5 m^{-1} and was associated with the low saline water from the Hudson River. The biological community responded to the sharp vertical gradients in the density measured during the upwelling periods, with phytoplankton as well as the bioluminescent organisms layering along the maximum stratification (Figures 4c and 4d). Bioluminescence ranged from background in the dense upwelled water to 3.7×10^{11} photons L^{-1} s^{-1} in the stratified layers. The time depth locations where there was a lack of correlation between phytoplankton and bioluminescence in time and space suggests a portion of the bioluminescent community consisted of heterotrophic dinoflagellates and/or zooplankton [Lapota, 1998; Moline et al., 2007]. In fact the

bioluminescent copepod Metridia lucens is found to be abundant in this region [Kane, 2003]. High phytoplankton loads were also evident periodically along the bottom during the deployment, resulting from particulate resuspension that occurs in this area during storms and/or intense upwelling [Agrawal, 2005].

--- INSERT FIGURE 5 ---

The water column sampled in 2001 showed very similar dynamics to 2001, with the physical data indicating upwelling conditions at the beginning and end of the deployment (Figure 5a). As in 2000, the density dropped by >0.5 kg m^{-3} on 1 August 2001 during the downwelling period, suggesting that the Hudson River influenced the sampling site. Peak attenuation c488 > 5 m^{-1} was associated with this fresh water influence as well as resuspension events that coincided with strong atmospheric forcing from the northeast (Figure 5b) [Moline et al., 2004]. These events also influenced the phytoplankton distributions (Figure 5b). Interestingly, the river signal was not proportionately high in phytoplankton suggesting the majority of the high attenuation signal as scattering particles. Mean bioluminescence for 2001 was similar to 2000, 1.6×10^9 versus 2.4×10^9 photons L^{-1} s^{-1}, however, the median values were lower for 2001 by an order of magnitude (3.1×10^8 versus 1.6×10^9 photons L^{-1} s^{-1}). This may indicate that zooplankton, which generally have higher flash intensities [Lapota and Losee, 1984], may have contributed more to the overall signal in 2001 than 2000. The large number of individual high intensity flashes 4–7 August 2001 between 7 and 12 m also suggest domination of the biological community by zooplankton (Figure 5d).

Variability in BL_w

--- INSERT FIGURE 6 ---

--- INSERT FIGURE 7 ---

As BL_w here is the maximum potential amount of water-leaving radiance from the bioluminescence source depth, BL_w from each depth reflects the relative changes in the structure of the

biological community and optical properties throughout the water column over both seasons (Figures 6 and 7). During 2000, BL_w was high due to high bioluminescence and relatively low uniform attenuation. As the bioluminescence stratified, the maximal water-leaving radiance at the surface was generated by MBP at 6 to 7 m, along the density gradients in response to the cold-water intrusion (Figure 4a). In mixed or downwelling conditions, the water-leaving radiance decreased exponentially with depth as both the light and the IOPs were similar throughout the water column. BL_w increased in the last three days of the deployment due to increasing bioluminescence along the pycnocline. Although total attenuation remained high during the day, attenuation measured at night decreased, presumably from decreased wind-driven mixing (Figure 4b). This allowed more photons generated deeper in the water column to propagate to the surface (Figure 6a). Despite slightly higher bioluminescence, BL_w in 2001 was approximately half that of 2000 as a result of high attenuation (Figure 7a). Attenuation generally increased while bioluminescence decreased, leading to a trended decrease in the BL_w over time (Figure 7a). The highest water-leaving radiance was 1.7×10^{-7} W m^{-2} sr^{-1} for 2 August 2000 with the mean BL_w for 2000 and 2001 of 6.8×10^{-9} and 1.5×10^{-9} W m^{-2} sr^{-1}, respectively. As with the MBP, the distribution of BL_w for 2001 was lower by an order of magnitude, with median values of 2.2×10^{-10} versus 1.5×10^{-9} W m^{-2} sr^{-1}. This implies the intensity range of BL_w is primarily driven by the intensity of MBP, with only same order variation from changes in IOPs.

Spectral Shift in BL_w

--- INSERT FIGURE 8 ---

As with the spectral shift in solar radiation with depth [Mobley, 1994], the modeled results of this study indicated a significant shift of >90 nm from blue to green as light propagates to the surface (Figure 8). The emission spectra of bioluminescent light measured in this study from organisms typical of coastal ecosystems, such as copepods and dinoflagellates, have an emission peak centered near ~475 nm (Figure 3). As the depth of the bioluminescence source increased, the proportion of BL_w at 474 nm relative to 555 nm decreased by up to 40-fold. The variation in the spectral shift with depth occurs in response to the

vertical structure of the measured IOPs. Figures 6b and 7b show the peak wavelength of the BL_w as a function of depth and time for 2000 and 2001, respectively. The most striking spectral differences occurred when the water column was optically stratified, with higher attenuating surface water and clearer bottom water. During these conditions, for example, 23 July 2000 and 2 August 2000, peak BL_w occurs in the blue wavelengths at nearly all depths. During downwelling conditions, maximum BL_w peak wavelengths (>540 nm) are from as shallow as 5 m (29 July 2000 and 4 August 2001).

Discussion

Variability in physical and optical dynamics has been well described for this study site [Glenn et al., 1996, 2004]. The variability in the local atmospheric forcing and influence of terrestrial runoff are the two largest contributors to the water column dynamics [Glenn et al., 2004; Oliver et al., 2004]. Alternating periods of upwelling and downwelling influenced by event-driven buoyant layers were captured in the present data set effecting the distribution of optical constituents, including phytoplankton, and the bioluminescent community. Consistent with previous findings, bioluminescence was most intense along strong vertical gradients in density set up from entrained bottom water [Widder et al., 1999; Moline et al., 2001]. The entrained bottom water itself showed the lowest bioluminescence intensity and beam attenuation c488. The similarity in the distributions of bioluminescence and phytoplankton weights generally indicate much of the bioluminescence was a result of autotrophic dinoflagellates and/or close aggregation of predator/prey fields [Moline et al., 2007]. The bio-optical responses were similar between the two years with influence of freshwater input at the end of both sampling periods. The highest optical load was contained in the fresher water and to a lesser extent in the surface waters throughout the study. This surface attenuation acted as a filter for the BL_w, however, the variability in MBP had the highest influence on the BL_w.

These findings from a single optically deep study area provide a quantitative picture of the significant variability in the BL_w over time and highlight the advantages simultaneous measurements of

bioluminescence potential and IOPs. HydroLight, as employed here, assumes a horizontally uniform layer of bioluminescence in the calculations. If bioluminescence is considered to be a point source function rather than a plane source function, then a Monte Carlo code could be used to incorporate the vertical and horizontal distribution of light and accurately predict water-leaving radiance as a function of horizontal position [Gordon, 1987]. The work of Gordon [1987] was part of the Biowatt/MLML programs, and illuminates the difficulties inherent in developing radiance models for bioluminescence water-leaving radiance, as well as possible difficulties in developing the sensors necessary to adequately measure BL_w. While this more rigorous approach may help to fully assess the modeled solution, the quantitative changes in BL_w presented here provide an opportunity to explore the sensitivities needed for detection of these events.

The development of shore-based, ship-based, and/or airborne low-light level (LLL) bioluminescence sensors have been identified as a need [Lynch, 1981; Lapota, 2003, 2005]. These sensors would not only need the appropriate sensitivities, but also have the spectral range required to quantify BL_w for bioluminescence stimulated at depth. There are a number of examples of remote detection of bioluminescence used to examine biological systems. Roithmayr [1970] used a low-light detector, called SANOS (Stabilization Airborne Night Observation System), aboard an aircraft at 1600 m to detect and map the distribution of bioluminescence associated with schools of Spanish mackerel off the coast of Florida. At the time this was seen as a tool for fishermen to reduce time required to locate productive fisheries, to map the sizes and distribution of schools for fisheries management, and to provide scientists an opportunity to study the behavior of fish schools at night. Miller et al. [2005] used the low-light Operational Linescan System on board a Defense Meteorological Satellite Program satellite to image bioluminescence from space for the first time. In this case, the bioluminescence signal was generated by a surface slick of bacteria extending over 15,100 Km^2 in the Indian Ocean. The spectral response of this sensor was not optimized for bioluminescence emissions, but demonstrates the opportunity to study this phenomenon in more detail. While surface events, such as this, are the most likely to be detected,

detection of bioluminescence subsurface requires increased sensitivities and, as this study suggests, spectral information.

--- INSERT FIGURE 9 ---

In order to expand the relevance and application of this study to other regions, the BL_w estimated from "stimulations" at geometric depths (Figures 6 and 7) is shown as a function of the optical depth tau ($\tau(\lambda)$, Figure 9), with

$$\tau\ (\lambda) = \int c\ (\lambda, z)\ dz, \qquad (1)$$

taking into account the depth dependent change in attenuation at wavelengths across the spectrum. BL_w as shown in Figure 9 is slightly different as it is the water-leaving radiance integrated over the 20 nm centered around the maximum wavelengths shown in Figures 6 and 7, and not over the entire spectrum, to simulate a spectral sensor's response. Although there is significant variability in BL_w, there is an expected decrease with increasing $\tau(\lambda)$ as well as increasing λ. The significant differentiation of τ with changing wavelengths suggests that spectral information may be used to delineate the depth of the bioluminescence source, and will be explored in part 2 of this paper [Oliver et al., 2007]. The range of $\tau(\lambda)$ further illustrates the high spectral attenuation at this site and allows these results to be portable to other locations. The spectral intensities of BL_w here also allow for examination of the sensitivities required to measure BL_w in an oceanographic context with current consumer off-the-shelf (COTS) technology.

Photomultiplier tubes, photodiodes and CCD image sensors are widely used for the detection of low level light and have been used in bioluminescent applications, both in water [Voss and Chapin, 1990; Widder et al., 1993, 2005; Herren et al., 2005; Moline et al., 2005] and above water [Roithmayr, 1970; Miller et al., 2005]. These detectors convert light into analog electrical signals. When the signal becomes too weak, however, so that the incident photons are detected as separate pulses, the single photon counting method using a PMT has higher detection efficiency and signal to noise (S/N) [Ingle and Powell, 1998; Hamamatsu Photonics, 2001]. A COTS single photon counter currently available (i.e., Hamamatsu

H7155) has dark counts (DC) per second, typically on the order of 50–100 per second. The S/N is observed at this detector placed at the focal point of a reflecting telescope. It is conservatively assumed that the telescope only collects light nadir from the source, from an area, A, of the ocean surface at some fixed height or distance, D. Deriving the S/N of the system works as follows:

$$\phi = \frac{BL_{\omega} \cdot A^2}{D^2}, \qquad (2)$$

where ϕ is the radiant flux in units of Watts from solid angle subtended by the ocean surface at the detector aperture. Dividing this by the energy carried by a photon of a given wavelength, gives the photon count (PC), or number of photons per second arriving at the detector from the ocean surface. Thus

$$PC = \frac{\phi\lambda}{hc} \qquad (3)$$

is essentially our result, since it is the number of photons arriving at the detector (the signal) per second. The S/N is then the ratio of PC to DC. For an aircraft at D = 1000 m, and a telescope with a 1 m diameter aperture, we compute that the S/N = $3.9 \times 10^{16} \cdot BL_w \cdot \lambda$. Assuming a S/N of 10 is conservatively a reasonable number for successful detection, the sensitivity of this example configuration would be 5.13×10^{-19} W m^{-2} sr^{-1}, with changes in λ not significantly influencing the sensitivity. Estimates of BL_w from this study were well above this detection level, even for the largest values of $\tau(\lambda)$ (Figure 9). This of course does not include interference light from anthropogenic sources or lunar radiance/reflection, which can significantly influence detection.

With current sensing technology and approaches indicating the possibility of detecting BL_w at the low intensities and range of wavelengths modeled in this study, the next step, detailed in part 2 of this paper [Oliver et al., 2007], is to examine using BL_w to predict the depth of a given bioluminescent event. High variability in c (λ) and MBP provided a large range of bio-optical conditions needed for robust evaluation. The combination of detection and prediction will begin to address the applied interests in

opportunities and hazards of bioluminescent events, and may be a powerful tool to assess biological communities in the ocean.

This study provides one of the first time series of the combined vertical structure of both IOPs and bioluminescence potential. While bioluminescent organisms represent a variable fraction of the total planktonic biomass, these data illustrate a community response to the episodic nature of this region. The cycle of upwelling and downwelling serve to provide alternating patterns of strong stratification followed by homogenous vertical water column. The biological communities responded to the stability with the highest bioluminescence measured in layers along the sharpest density gradients, produced by entrained offshore waters. Downwelling periods produced minimal gradients with communities correspondingly distributed throughout the water column. Depending on the intensity of downwelling and/or vertical mixing, vertical migration by autotrophic and/or heterotrophic plankton produced some organization of the community. These highly resolved dynamics demonstrate bioluminescence as a useful measure in delineating planktonic community response to environmental fluctuation. Expanded use of bioluminescence as a standard oceanographic measure may afford the oceanographic community new ways to observe (both in situ and above water) and to improve understanding of planktonic communities in the ocean.

Acknowledgments

We wish to thank M. Purcell, C. Von Alt, and C. Johnson for fabrication of the optical profiler, the Rutgers Marine Field Station and R/V Arabella staff for deployment, and S. Glenn for the ocean observation infrastructure at Rutgers University. Profiler operators were J. Blackwell, S. Blackwell, A. Briggs, G. Chang, M. Crowley, J. Kohut, K. Oliver, J. Pearson, D. Peterson, and A. Weidemann. This study was funded by ONR (N00014-99-1-0197, N00014-00-1-0008, and N00014-03-1-0341 to M. Moline, N00014-97-0767 and N00014-99-1-0196 to O. M. E. Schofield, and N00014-04-M-0108 to C. D. Mobley) and the National Ocean Partnership Program (N00014-97-1-1019).

References

Abrahams, V. A., and L. D. Townsend (1993), Bioluminescence in dinoflagellates: A test of the burglar alarm hypothesis, Ecology, 74, 258–260.

Agrawal, Y. C. (2005), The optical volume scattering function: Temporal and vertical variability in the water column off the New Jersey coast, Limnol. Oceanogr., 50(6), 1787–1794.

Alberte, R. S. (1993), Bioluminescence: The fascination, phenomena, and fundamentals, Naval Res. Rev., 45, 2–12.

Batchelder, H. P., E. Swift, and J. R. van Keuren (1990), Patterns of planktonic bioluminescence in the northern Sargasso Sea: Seasonal and vertical distribution, Mar. Biol., 104, 153–164.

Batchelder, H. P., E. Swift, and J. R. van Keuren (1992), Diel patterns of planktonic bioluminescence in the northern Sargasso Sea, Mar. Biol., 113, 329–339.

Burkenroad, M. D. (1943), A possible function of bioluminescence, J. Mar. Res., 5, 161–164.

Carder, K. L., Z. P. Lee, J. Marra, R. G. Steward, and M. J. Perry (1995), Calculated quantum yield of photosynthesis of phytoplankton in the Marine Light-Mixed Layers (59°N, 21°W), J. Geophys. Res., 100, 6655–6664.

Case, J. F., E. A. Widder, S. Bernsein, K. Ferer, D. Young, M. I. Latz, M. Geiger, and D. Lapota (1993), Assessment of marine bioluminescence, Naval Res. Rev., 45, 31–41.

Cussatlegras, A., P. Geistdoerfer, and L. Prieur (2001), Planktonic bioluminescence measurements in the frontal zone of Almeria-Oran (Mediterranean Sea), Oceanologica, 24, 239–250.

Dickey, T., et al. (1993), Seasonal variability of bio-optical and physical properties in the Sargasso Sea, J. Geophys. Res., 98, 865–898.

Franks, P. J. S. (1992a), Phytoplankton blooms at fronts: Patterns, scales, and physical forcing mechanisms, Rev, Aquat. Sci., 6, 121–137.

Franks, P. J. S. (1992b), Sink or swim: Accumulation of biomass at fronts, Mar. Ecol. Prog. Ser., 82, 1–12.

Franks, P. J. S. (1995), Thin layers of phytoplankton: A model of formation by near-inertial wave shear, Deep Sea Res., Part I, 42, 75–91.

Franks, P. J. S., and C. Chen (1996), Plankton production in tidal fronts: A model of Georges Bank in summer, J. Mar. Res., 54, 631–651.

Glenn, S. M., M. F. Crowley, D. B. Haidvogel, and Y. T. Song (1996), Underwater observatory captures coastal upwelling events off New Jersey, Eos Trans. AGU, 77, 233–236.

Glenn, S., et al. (2004), Biogeochemical impact of summertime coastal upwelling on the New Jersey Shelf, J. Geophys. Res., 109, C12S02, doi:10.1029/2003JC002265.

Gordon, H. R. (1987), Bio-optical model describing the distribution of irradiance at the sea surface resulting from a point source embedded in the ocean, Appl. Opt., 26, 4133–4148.

Hamamatsu Photonics (2001), Photon counting using photomultiplier tubes, Tech. Inf. Rep. TPHO9001E03, Hamamatsu City, Japan.

Hastings, J. W. (1983), Biological diversity, chemical mechanisms, and the evolutionary origins of bioluminescent systems, J. Mol. Evol., 19, 309–321.

Hastings, J. W., and K. H. Nealson (1977), Bacterial bioluminescence, Annu. Rev. Microbiol., 31, 549–595.

Herren, C. M., S. H. D. Haddock, C. Johnson, C. Orrico, M. A. Moline, and J. F. Case (2005), A multi-platform bathyphotometer for fine-scale, coastal bioluminescence research, Limnol. Oceanogr. Methods, 3, 247–262.

Herring, P. J. (1987), Systematic distribution of bioluminescence in living organisms, J. Bioluminesc. Chemiluminesc., 1, 147–163.

Ingle, M. B., and J. R. Powell (1998), Advances in photon counting for bioluminescence, in Image Intensifiers and Applications; and Characteristics and Consequences of Space Debris and Near-Earth Objects, edited by C. B. Johnson et al., Proc. SPIE Int. Soc. Opt. Eng., 3434, 56–61.

Kane, J. (2003), Spatial and temporal abundance patterns for the late stage copepodites of Metridia lucens (Copepoda: Calanoida) in the U.S. northeast continental shelf ecosystem, J. Plankton Res., 25, 151–167.

Lapota, D. (1998), Long term and seasonal changes in dinoflagellate bioluminescence in the Southern California Bight, Ph.D. thesis, 193 pp., Univ. of Calif. Santa Barbara, Santa Barbara, 28 June.

Lapota, D. (2003), Buoy-mounted bioluminescence sensor (BioBuoy) for special operations, Tech. Doc. 3155, pp. 142–145, Space and Naval Warfare Cent., San Diego, Calif.

Lapota, D. (2005), Night time surveillance of harbors and coastal areas using bioluminescence camera and buoy systems, in Photonics for Port and Harbor Security, edited by M. J. DeWeert and T. T. Saito, Proc. SPIE Int. Soc. Opt. Eng., 5780, 128–137.

Lapota, D., and J. R. Losee (1984), Observations of bioluminescence in marine plankton from the Sea of Cortez, J. Exp. Mar. Biol. Ecol., 77, 209–240.

Lapota, D., C. Galt, J. Losee, H. D. Huddell, J. K. Orzech, and K. H. Nealson (1988), Observations and measurements of planktonic bioluminescence in and around a milky sea, J. Exp. Mar. Biol. Ecol., 119, 55–81.

Lapota, D., M. L. Geiger, A. V. Stiffey, D. E. Rosenberger, and D. K. Young (1989), Correlations of planktonic bioluminescence with other oceanographic parameters from a Norwegian fjord, Mar. Ecol. Prog. Ser., 55, 217–227.

Lapota, D., D. E. Rosenberger, and S. H. Lieberman (1992), Planktonic bioluminescence in the pack ice and the marginal ice zone of the Beaufort Sea, Mar. Biol., 112, 665–675.

Latz, M. I., T. M. Frank, M. R. Bowlby, E. A. Widder, and J. F. Case (1987), Variability in flash characteristics of a bioluminescent copepod, Biol. Bull., 162, 423–448.

Latz, M. I., T. M. Frank, and J. F. Case (1988), Spectral composition of bioluminescence of epipelagic organisms from the Sargasso Sea, Mar. Biol., 98, 441–446.

Lynch, R. V. (1981), Patterns of bioluminescence in the oceans, NRL Rep. 8475, 32 pp., Naval Res. Lab., Washington, D. C.

Marra, J., and E. O. Hartwig (1984), Biowatt: A study of bioluminescence and optical variability in the sea, Eos Trans. AGU, 65, 732–733.

Marra, J., C. Langdon, and C. A. Knudson (1995), Primary production, water column changes, and the demise of a Phaeocystis bloom at the Marine Light–Mixed Layers site (59°N, 21°W) in the northeast Atlantic Ocean, J. Geophys. Res., 100(C4), 6633–6644.

Miller, S. D., S. H. D. Haddock, C. D. Elvidge, and T. F. Lee (2005), Detection of a bioluminescent milky sea from space, Proc. Natl. Acad. Sci. U. S. A., 102, 14,181–14,184.

Mobley, C. D. (1994), Light and Water: Radiative Transfer in Natural Waters, 592 pp., Academic, New York.

Mobley, C. D., and L. K. Sundman (2001a), HydroLight 4.2 Users' Guide, Sequoia Sci., Inc., Mercer Island, Wash. (Available at http://www.HydroLight.info)

Mobley, C. D., and L. K. Sundman (2001b), HydroLight 4.2 Technical Documentation, Sequoia Sci., Inc., Mercer Island, Wash. (Available at http://www.HydroLight.info)

Moline, M. A., E. Heine, J. Case, C. Herren, and O. Schofield (2001), Spatial and temporal variability of bioluminescence potential in coastal regions, in Bioluminescence and Chemiluminescence 2000, edited by J. F. Case et al., pp. 123–126, World Sci., Singapore.

Moline, M. A., S. M. Blackwell, R. Chant, M. J. Oliver, T. Bergmann, S. Glenn, and O. M. E. Schofield (2004), Episodic physical forcing and the structure of phytoplankton communities in the coastal waters of New Jersey, J. Geophys. Res., 109, C12S05, doi:10.1029/2003JC001985.

Moline, M. A., S. M. Blackwell, B. Allen, T. Austin, N. Forrester, R. Goldsborough, M. Purcell, R. Stokey, and C. von Alt (2005), Remote Environmental Monitoring UnitS: An autonomous vehicle for characterizing coastal environments, J. Atmos. Oceanic Technol., 22(11), 1798–1809.

Moline, M. A., S. M. Blackwell, J. F. Case, S. H. D. Haddock, C. M. Herren, C. M. Orrico, and E. Terrill (2007), Bioluminescence to reveal structure and interaction of coastal planktonic communities, Deep Sea Res., Part I, in press.

Morin, J. G. (1983), Coastal bioluminescence: Patterns and functions, Bull. Mar. Sci., 33(4), 787–817.

Morin, J. G., and A. C. Cohen (1991), Bioluminescent displays, courtship, and reproduction in ostracodes, in Crustacean Sexual Biology, edited by R. Bauer and J. Martin, pp. 1–16, Columbia Univ. Press, New York.

Nealson, K. H. (1993), Bacterial bioluminescence: Three decades of enlightenment, Naval Res. Rev., 45, 13–30.

Oliver, M. J., O. Schofield, T. Bergmann, S. Glenn, C. Orrico, and M. Moline (2004), Deriving in situ phytoplankton absorption for bio-optical productivity models in turbid waters, J. Geophys. Res., 109, C07S11, doi:10.1029/2002JC001627.

Oliver, M. J., M. A. Moline, C. D. Mobley, L. Sundman, and O. M. E. Schofield (2007), Bioluminescence in a complex coastal environment: 2. Prediction of bioluminescent source depth from spectral water-leaving radiance, J. Geophys. Res., doi:10.1029/2007JC004136, in press.

Ondercin, D. G., C. A. Atkinson, and D. A. Kiefer (1995), The distribution of bioluminescence and chlorophyll during the late summer in the North Atlantic: Maps and a predictive model, J. Geophys. Res., 100, 6575–6590.

Pegau, W., D. Gray, and J. Zaneveld (1997), Absorption and attenuation of visible and near-infrared light in water: Dependence on temperature and salinity, Appl. Optics, 36(24), 6035–6046.

Petzold, T. J. (1972), Volume scattering functions for selected ocean waters, Tech. Rep. SIO, pp. 72–78, Scripps Inst. of Oceanogr., San Diego, Calif.

Pope, R. M., and E. S. Fry (1997), Absorption spectrum (380–700 nm) of pure water. II. Integrating cavity measurements, Appl. Opt., 36, 8710–8723.

Rohr, J., M. I. Latz, S. Fallon, J. C. Nauen, and E. Hendricks (1998), Experimental approaches towards interpreting dolphin-stimulated bioluminescence, J. Exp. Biol., 201, 1447–1460.

Roithmayr, C. M. (1970), Airborne low-light sensor detects luminescing fish schools at night, Commer. Fish. Rev., 32, 42–51.

Schofield, O., T. Bergmann, M. J. Oliver, A. Irwin, G. Kirkpatrick, W. P. Bissett, M. A. Moline, and C. Orrico (2004), Inversion of spectral absorption in the optically complex coastal waters of the Mid-Atlantic Bight, J. Geophys. Res., 109, C12S04, doi:10.1029/2003JC002071.

Seliger, H. H., W. G. Fastie, and W. D. McElroy (1969), Towable photometer for rapid area mapping of concentrations of bioluminescent marine dinoflagellates, Limnol. Oceanogr., 14, 806–813.

Smith, R. C., J. Marra, M. J. Perry, K. S. Baker, E. Swift, E. Buskey, and D. A. Kiefer (1989), Estimation of a photon budget for the upper ocean in the Sargasso Sea, Limnol. Oceanogr., 34, 1673–1693.

Stramska, M., T. D. Dickey, A. Plueddlemann, R. Weller, C. Langdon, and J. Marra (1995), Bio-optical variability associated with phytoplankton dynamics in the North Atlantic Ocean during spring and summer of 1991, J. Geophys. Res., 100, 6621–6632.

Swift, E., J. M. Sullivan, H. P. Batchelder, J. Van Keuren, R. D. Vaillancourt, and R. R. Bidgare (1995), Bioluminescent organisms and bioluminescence measurements in the North Atlantic Ocean near latitude 59.°5N, longitude 21°W, J. Geophys. Res., 100, 6527–6547.

Voss, K. J., and A. L. Chapin (1990), Measurement of the point spread function in the ocean, Appl. Opt., 29, 3638–3642.

Widder, E. A., J. F. Case, S. A. Bernstein, S. MacIntyre, M. R. Lowenstine, M. R. Bowlby, and D. P. Cook (1993), A new large volume bioluminescence bathyphotometer with defined turbulence excitation, Deep Sea Res., Part I, 40, 607–627.

Widder, E. A., S. Johnson, S. A. Bernstein, J. F. Case, and D. J. Neilson (1999), Thin layers of bioluminescent copepods found at density discontinuities in the water column, Mar. Biol., 134, 429–437.

Widder, E. A., C. L. Frey, and J. R. Bowers (2005), Improved bioluminescence measurement instrument, Sea Technol., 46(2), 10–16.

Zaneveld, J., and J. Kitchen (1994), The scattering error correction of reflecting tube absorption meters, Proc. SPIE Int. Soc. Opt. Eng., 2258, 44–55.

Figures

Figure 1

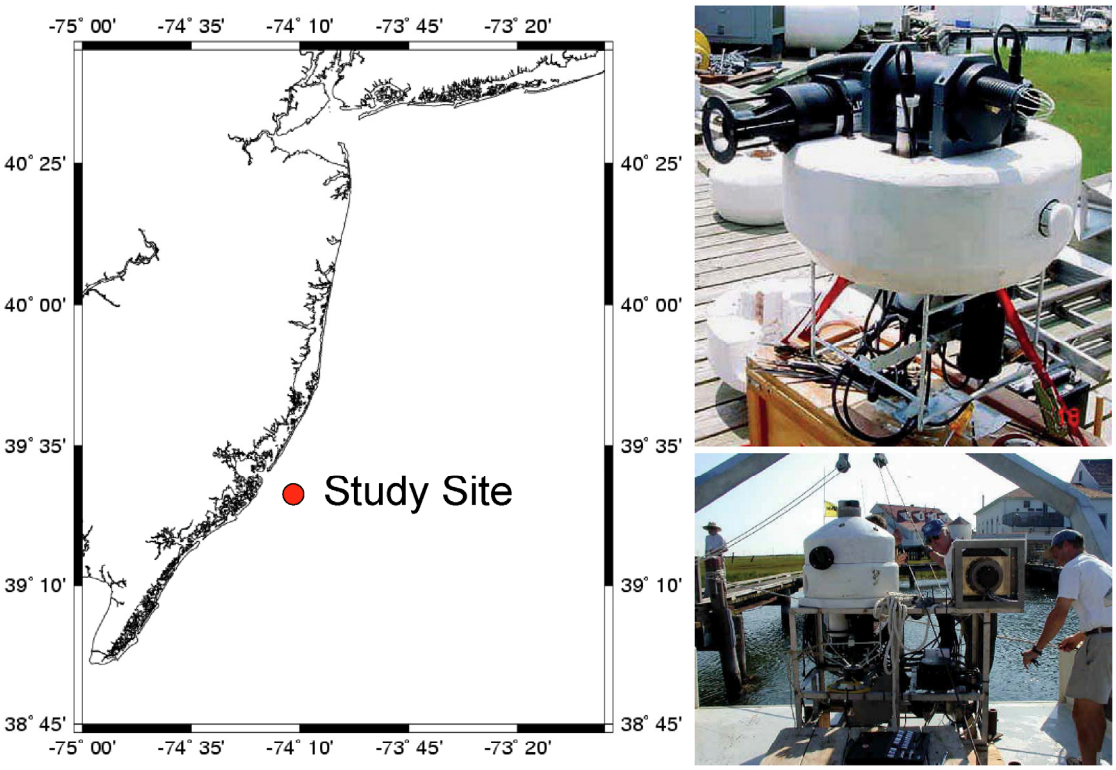

Figure 1. Location of study site along the New Jersey coastline. The instruments used in this study were attached to a profiling frame and embedded in a floating drogue (top right). This frame was attached by a winch to the profiler (bottom right) deployed on the ocean floor. Pictured is one of two profilers used in this study that received power and had real-time telemetry via an electro fiber-optic cable connected to shore.

Figure 2

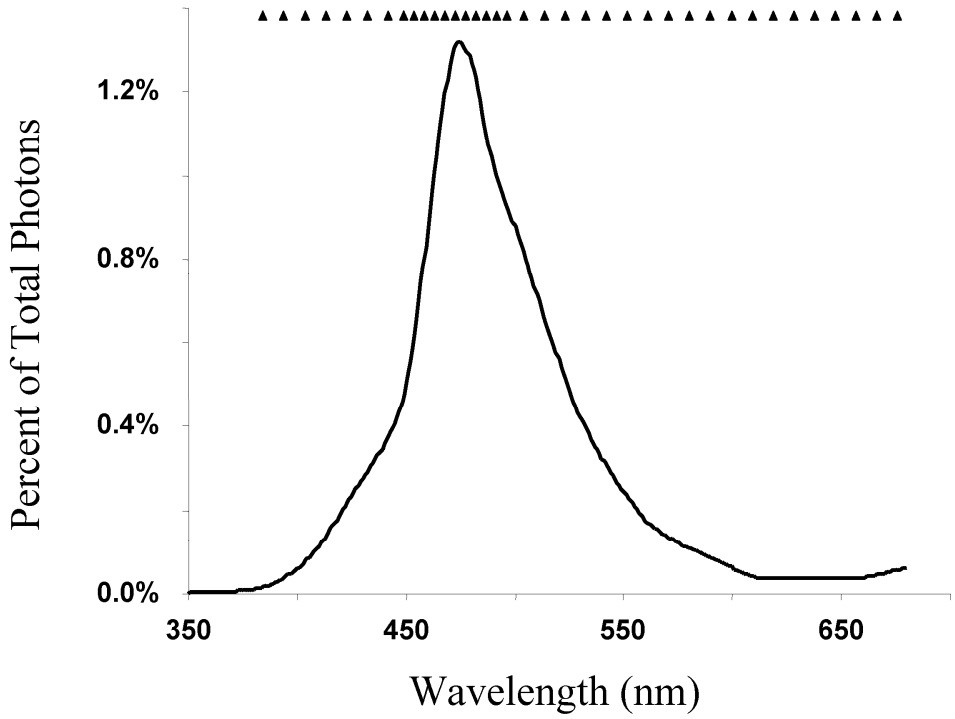

Figure 2. Bioluminescence spectrum used as input for the RTE model HydroLight. The diamonds above indicate the 37 modeled wavelengths for this study. Data for this spectrum were from bioluminescent phytoplankton and copepods isolated and measured in a spectral luminescence sphere. The weight of each biological component was based on the observed abundances as well as the bioluminescence emission patterns [Moline et al., 2007].

Figure 3

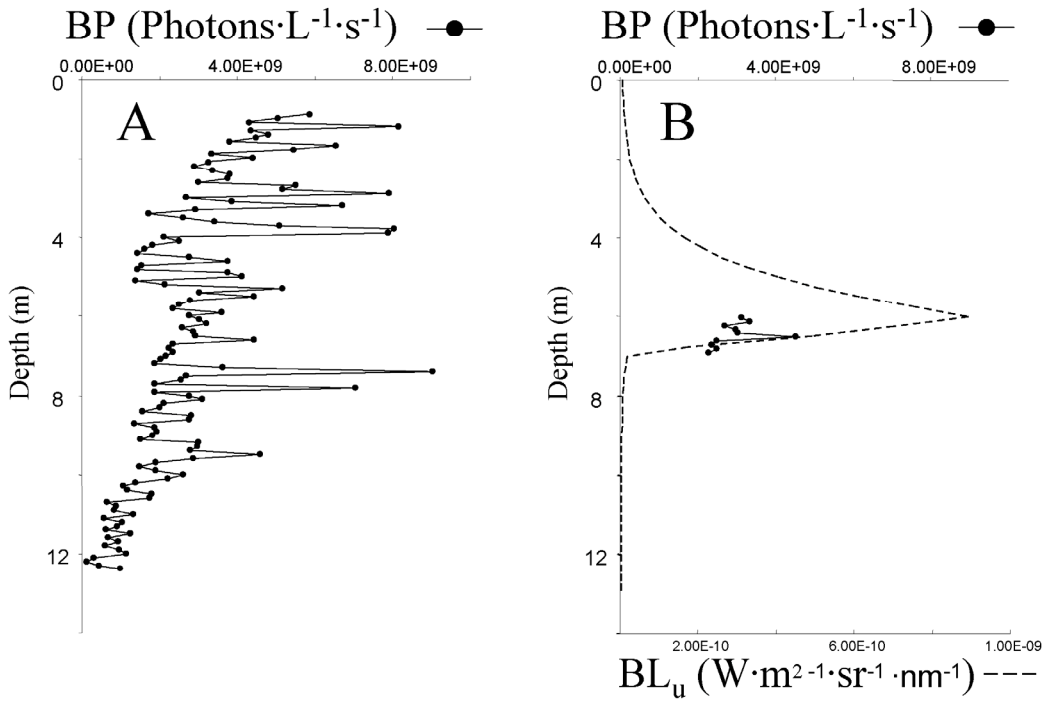

Figure 3. (a) A mechanically stimulated bioluminescence potential (MBP) profile taken 3 August 2001. (b) Using the bioluminescence measured between 6 and 7 m, the HydroLight RTE model propagates the radiance (dashed line) from that "stimulation" to the surface. This example is shown for 487.5 nm, one of 37 wavelengths modeled from the bioluminescence spectra (Figure 2).

Figure 4

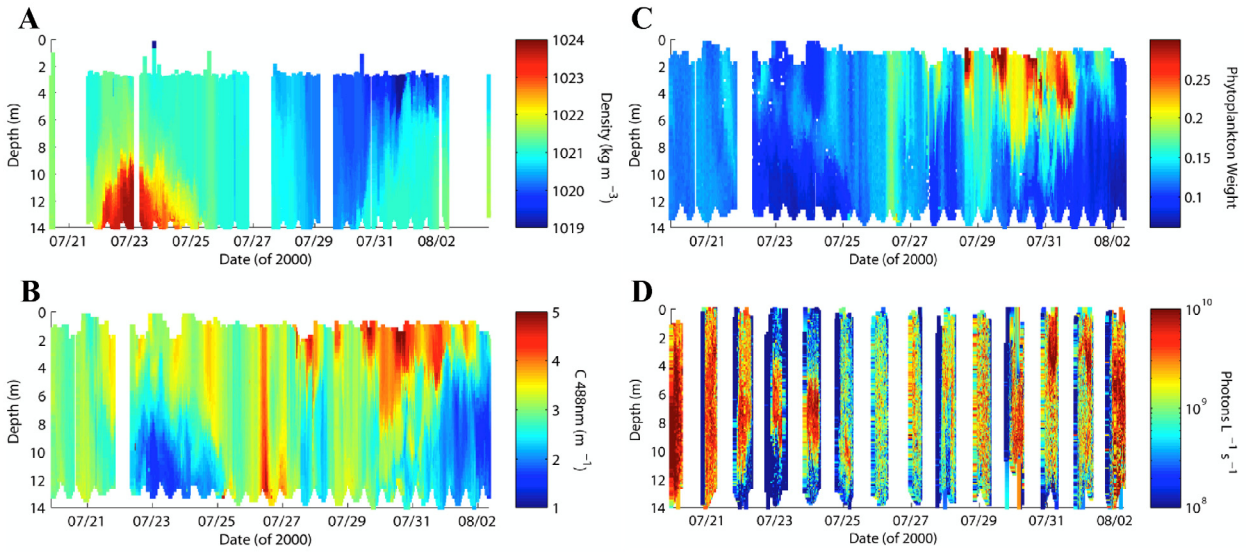

Figure 4. Time series of the depth distribution of (a) density (kg m^{-3}), (b) attenuation at 488 nm (m^{-1}), (c) phytoplankton weight, and (d) mechanically stimulated bioluminescence potential (photons L^{-1} s^{-1}) for 2000. Phytoplankton weights were calculated on the basis of optical deconvolution of spectral absorption detailed by Schofield et al. [2004].

Figure 5

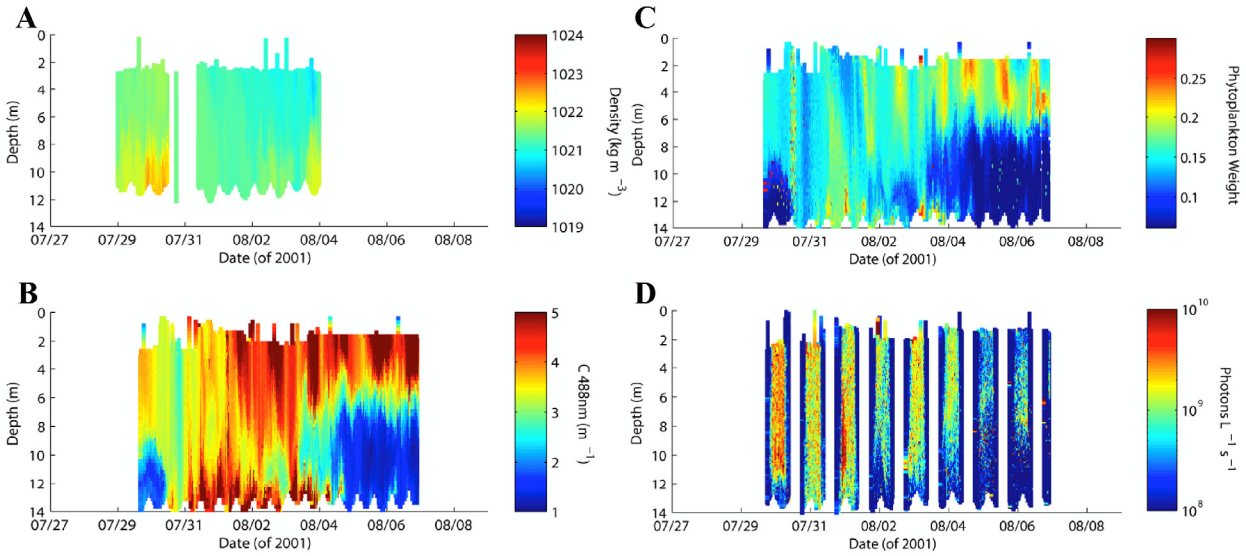

Figure 5. Time series of the depth distribution of (a) density (kg m−3), (b) attenuation at 488 nm (m−1), (c) phytoplankton weight, and (d) mechanically stimulated bioluminescence potential (photons L−1 s−1) for 2001. Phytoplankton weights were calculated on the basis of optical deconvolution of spectral absorption detailed by Schofield et al. [2004].

Figure 6

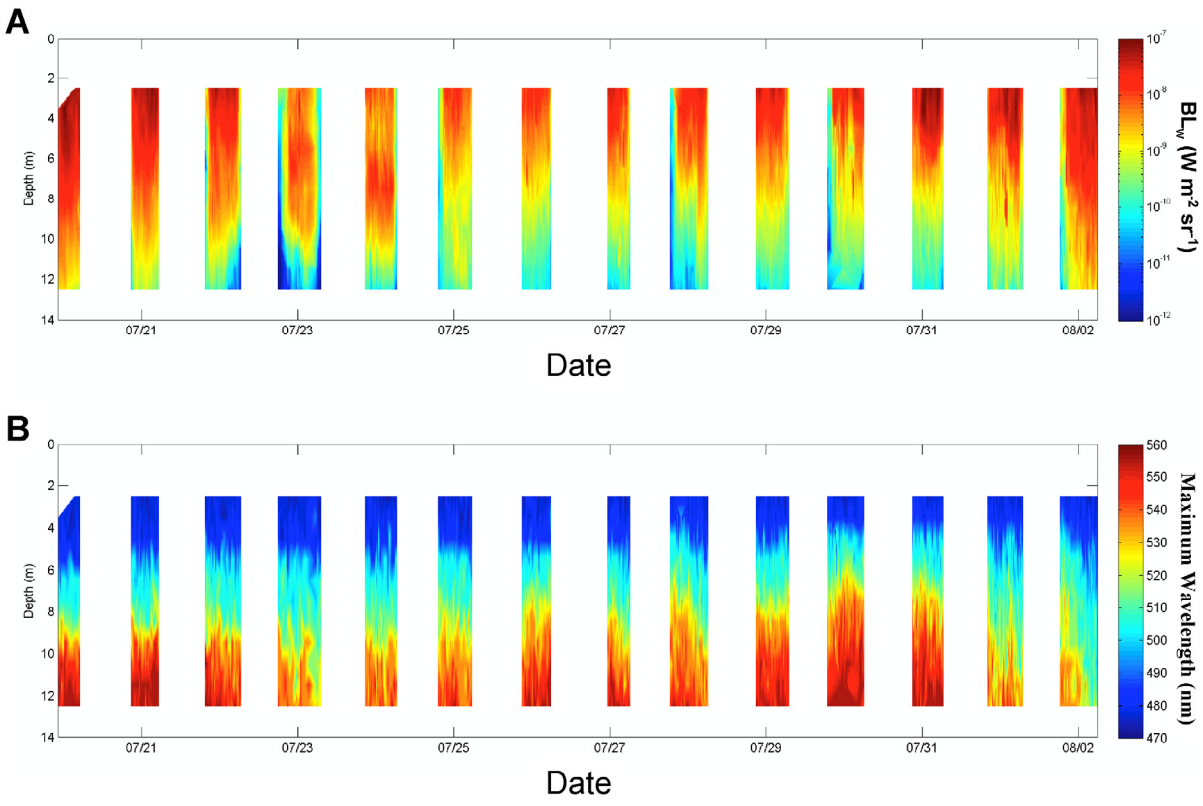

Figure 6. Time series of (a) the modeled surface bioluminescence water-leaving radiance (BLw; W m−2 sr−1) for mechanically stimulated bioluminescence at depth and (b) the maximum wavelength (nm) of the BLw from that depth. BLw is spectral water-leaving radiance in the nadir-viewing direction integrated over all wavelengths shown in Figure 2. Data are from 2000 using data shown in Figure 5.

Figure 7

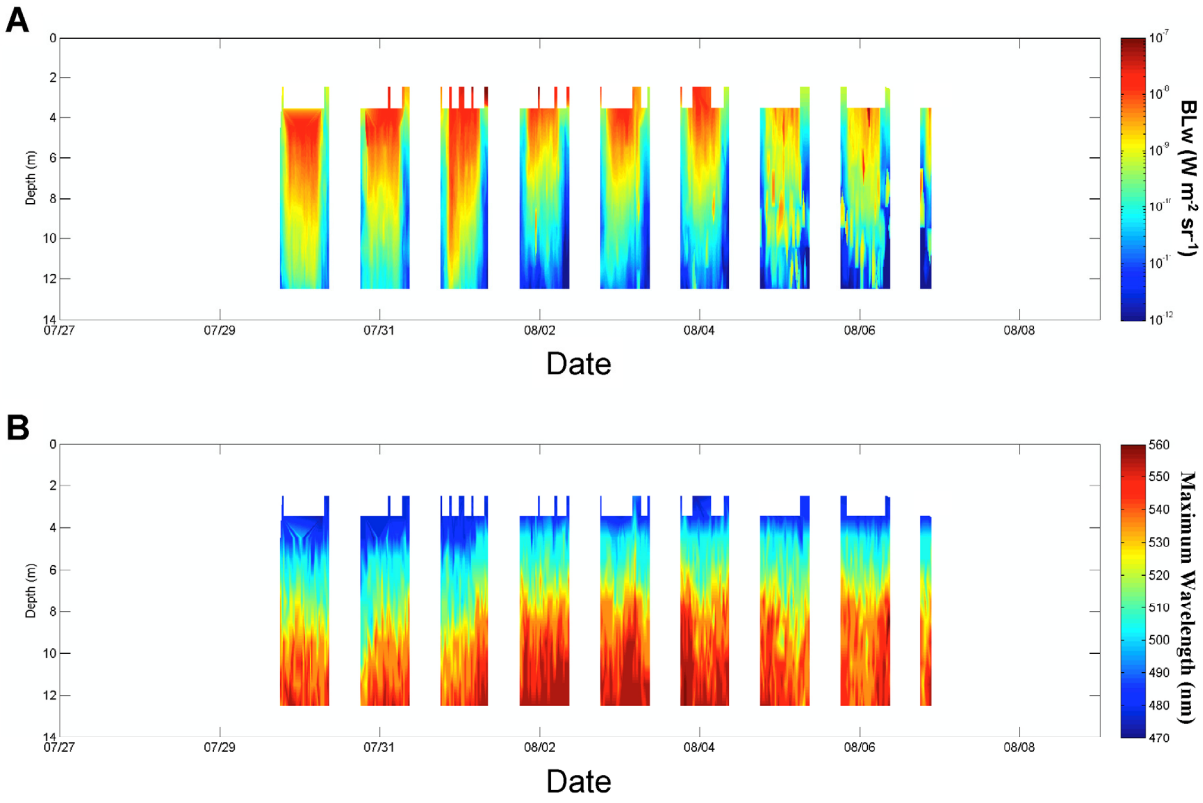

Figure 7. Time series of (a) the modeled surface bioluminescence water-leaving radiance (BL_w; W m^{-2} sr^{-1}) for mechanically stimulated bioluminescence at depth and (b) the maximum wavelength (nm) of the BL_w from that depth. BL_w is spectral water-leaving radiance in the nadir-viewing direction integrated over all wavelengths shown in Figure 2. Data are from 2001 using data shown in Figure 5.

Figure 8

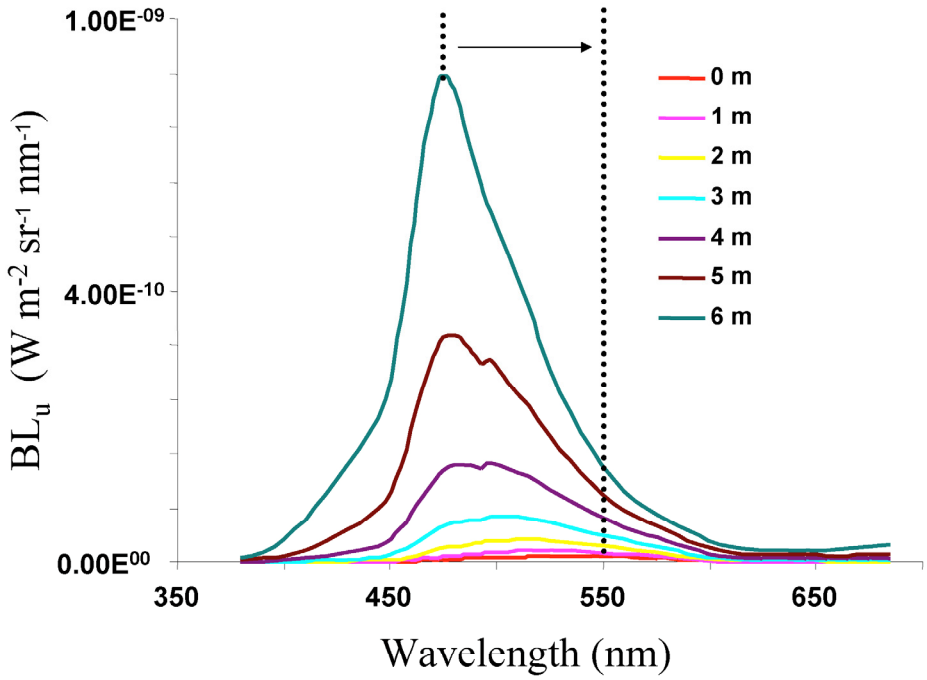

Figure 8. Example of the shift in the maximum wavelength of the upward bioluminescence radiance from data shown in Figure 3.

Figure 9

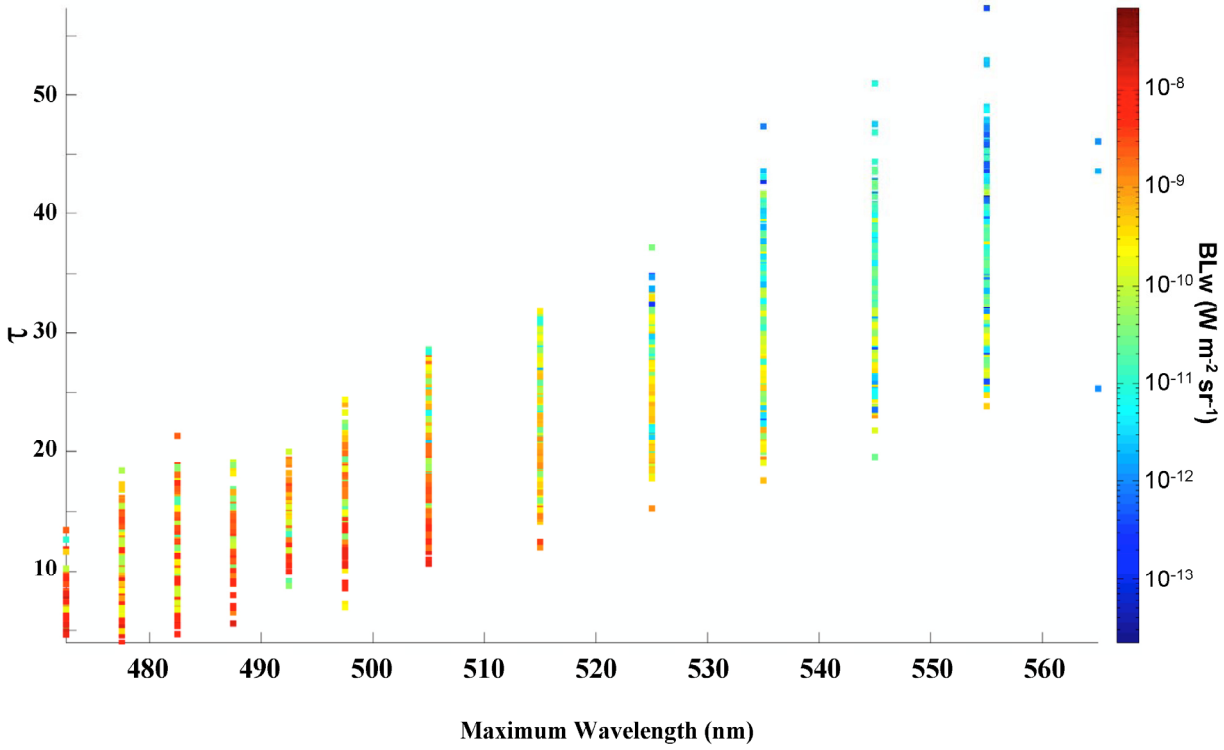

Figure 9. Distribution the modeled surface bioluminescence water-leaving radiance (BLw; W m−2 sr−1) from 2000 and 2001 as a function of the optical path length (τ) and maximum wavelength (nm). BLw values in this figure are integrated only in a 20 nm full width at half the maximum wavelength shown for detection applications.